EPR study of the role of ionic displacement on the ferroelastic-antiferroelectric transition of $KD_3(SeO_3)_2$

J. C. Machado da Silva, A. S. Chaves, R. Gazzinelli, and G. M. Ribeiro
Departamento de Física, ICEx, Universidade Federal de Minas Gerais, C.P. 702 - Belo Horizonte, Brazil

R. Blinc and I. Zupancic
Josef Stefan Institute, University of Ljubljana, Ljubljana, Yugoslavia

(Received 2 June 1980)

The electron paramagnetic resonance of the SeO_2^- center in $KD_3(SeO_3)_2$ was investigated in the temperature range -170–$+80$ °C. The orientation of the g tensor shows that the defect is essentially an O_2^- molecule perturbed by the Se in its equatorial plane. Four chemically equivalent sites were found in the paraelastic phase; the resonance lines corresponding to each site split in two lines in the ferroelastic phase due to rotations of the SeO_2^- centers in opposite domains. The line which connects the two oxygens rotates 4.1° around one of the $(0, \pm\sqrt{2}/2, \pm\sqrt{2}/2)$ axes at -150 °C. The rotations are proportional to $(T_c - T)^{1/2}$, allowing the conclusion that they are linearly coupled to the order parameter. The eigenvalues of the g tensors were found to be slightly different for the corresponding sites in opposite domains; this was interpreted as an indication that the crystal is pyroelectric. Weak lines appearing near each SeO_2^- resonance line were interpreted as being due to correlated SeO_2^- centers resulting from the extremely high concentration of these defects.

I. INTRODUCTION

It is well known[1–10] that $KH_3(SeO_3)_2$ (KTS) and $KD_3(SeO_3)_2$ (DKTS) undergo second-order phase transitions from a high-temperature orthorhombic ($Pbcn - D_{2h}^{14}$) to a low-temperature monoclinic phase ($P2_1/b - C_{2h}^5$) at the temperatures 211.7 and ~301 K, respectively. The transitions are associated with an instability of the B_{3g} acoustic phonon at the Γ point of the Brillouin zone and the onset of a shear strain σ_4 in the bc plane which is the condensed B_{3g} acoustic mode.

A displacive transition induced by an optical mode has a small transition entropy which results from the quantum-mechanical correction in the energy stored in the soft mode, $E = m\omega_{sm}^2\langle Q^2\rangle$, as the frequency ω_{sm} goes to zero. The transition entropy in a ferroelastic transition is expected to be even smaller, since the acoustic mode, due to its small frequency, can be treated classically for all temperatures. However, the transition entropy for KTS is quite large, 0.59 cal mol^{-1} K^{-1}.[11] Furthermore, a pure ferroelastic transition, i.e., a transition involving only the acoustic mode, is expected to have a very small transition temperature shift with deuteration, due to the change in the mass density, while in KTS T_c changes from 211.7 to ~301 K with deuteration. These facts plus the existence of positionally disordered protons in KTS at room temperature, found by Lechmann and Larsen[6] led Makita *et al.*[11,12] to propose that in addition to the shear strain, there is also the condensation of a proton mode associated with the phase transition in KTS. This mode necessarily has B_{3g} symmetry and consequently is nonpolar, which means that its condensation causes an antiferroelectric ordering of the protons. Thus, KTS is possibly the first known system to be simultaneously ferroelastic and antiferroelectric. It would also be the first known example of an antiferroelectric transition at the Γ point of the Brillouin zone (antiferroelectric ferrodistortive transition).

The elastic, dielectric, and thermal macroscopic properties of KTS are well described by a free energy density involving the linear coupling between σ_4 and a transition parameter Q, presumably related to the protons[11,12]

$$F(Q,\sigma_\lambda,P_i) = F_0 + \tfrac{1}{2}\alpha Q^2 + \tfrac{1}{4}\beta_1 Q^4 + \gamma\sigma_4 Q + \tfrac{1}{2}c_{44}^0\sigma_4^2 + \tfrac{1}{4}\beta_2\sigma_4^4 + \tfrac{1}{2}\sum_{i,j=1}^{3} c_{ij}^0\sigma_i\sigma_j + \tfrac{1}{2}\sum_{k=5}^{6} c_{kk}^0\sigma_k^2 + \sum_{i=1}^{3}(\eta_i Q^2 + \delta_i\delta_4^2)\sigma_i + (\eta_4 Q + \delta_4\sigma_4)\sigma_5\sigma_6 + F_p \ , \quad (1)$$

$$F_p = \tfrac{1}{2}\sum_{i=1}^{3}(\chi_{ii}^0)^{-1}P_i^2 + (\lambda_4 Q + \mu_4\sigma_4)P_2P_3 + \sum_{i=1}^{3}(\lambda_i Q^2 + \mu_i\sigma_4^2)P_i^2 \ ,$$

where P_i are the components of the electrical polarization.

The known properties of the crystal can be explained with two distinct hypotheses about the temperature variation of the coefficients in expression (1): (i) $\alpha = \alpha'(T - T_0)$, all other coefficients being constant; and (ii) $c_{44}^0 = C'(T - T_0)$, all other coefficients being constant. According to hypothesis (i) the driving force which causes the phase transition is the variable Q; i.e., the crystal is a proper antiferroelectric and improper ferroelastic. According to hypothesis (ii) the crystal is a proper ferroelastic and improper antiferroelectric. The true nature of the parameter Q and the two possibilities discussed above are questions still open to investigation. Very recently, Pick[13] observed a soft optical mode whose frequency extrapolates to zero at a temperature below T_c. This fact is easier to explain with hypothesis (i). A theoretical microscopic analysis of the problem has recently been made.[14]

Figure 1 shows the projection of the high-temperature phase structure of KTS on the *ac* plane. The disordered protons determined by Lehmann and Larsen[6] are shown. It is seen that the unit cell has four formula units and, consequently, eight SeO_3 radicals; they are numbered in the figure. The symmetry operations within the cell of the D_{2h}^{14} space group of KTS are[10]: E, $\{C_2^x/\vec{t}_1\}$, $\{C_2^y/\vec{t}_2\}$, $\{C_2^z/\vec{t}_3\}$, 1, $\{\sigma_x/\vec{t}_1\}$, $\{\sigma_y/\vec{t}_2\}$, $\{\sigma_z/\vec{t}_3\}$, where $\vec{t}_1 = \frac{1}{2}(\vec{a} + \vec{b})$, $\vec{t}_2 = \frac{1}{2}\vec{c}$, and $\vec{t}_3 = \frac{1}{2}(\vec{a} + \vec{b} + \vec{c})$. For the C_{2h}^5 space group they are: E, $\{C_2^x/\vec{t}_1\}$, 1, and $\{\sigma_x/\vec{t}_1\}$.

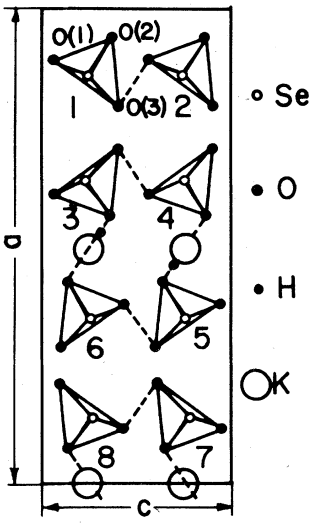

FIG. 1. Structure of paraelastic phase of KTS and DKTS; projection on *ac* plane. Dashed lines with small dots show the disordered hydrogen bonds determined by Lehmann and Larsen (Ref. 6).

Thus, in the D_{2h} phase the radical number 1 can move to the position of any other radical by a symmetry operation, which means that all eight SeO_3 radicals are in chemically equivalent sites. There are eight physically inequivalent sites, but site 1 goes to site 7, site 4 goes to site 6, etc., by inversion, which means that there are only four magnetically inequivalent sites. In the C_{2h} phase the odd-numbered sites become chemically distinct from the even-numbered ones. The situation is similar to what happens in $RbH_3(SeO_3)_2$, where there is only one chemically distinct site at high temperatures (paraelectric phase) and two chemically distinct sites at low temperatures, and contrasts with what happens in $NaH_3(SeO_3)$ and $LiH_3(SeO_3)_2$, which have two chemically inequivalent sites at all temperatures.

This paper presents the results of an electron-paramagnetic-resonance (EPR) investigation of the role of the lattice ions in the phase transition of DKTS, employing x-irradiated samples. We particularly wanted to answer the following questions:

(i) Do the lattice ions participate in the phase transition?

(ii) What is the nature of the ionic displacements and how do they vary with the order parameter?

(iii) Are the lattice ions sensitive to soft-mode or to central-peak-type fluctuations?

A previous EPR investigation of irradiated[15] and a neutron diffraction study of DKTS[16] have shown that the ions do indeed participate in the phase transition but have left the other questions unanswered. A preliminary report of the present investigation has been published.[17]

II. EXPERIMENTAL RESULTS AND DISCUSSIONS

Samples with ~90% deuteration and $T_c = 294$ K were employed in the experiments. Similarly to what happens with $NaH_3(SeO_3)_2$,[18] $LiH_3(SeO_3)_2$,[19] and $RbH_3(SeO_3)_2$, (Ref. 20) stable SeO_2^- radicals[21] are created with extraordinary efficiency by x irradiation at room temperature.

The distances between the ions Se, O(1), O(2), and O(3) of the group SeO_3 at room temperature are given in Table I for DKTS. The table shows that O(3) is more weakly bound to the cluster and conse-

TABLE I. Se–O distances in the SeO_3 radical. Data from Ref. 6.

Se–O(1)	1.661 Å
Se–O(2)	1.716 Å
Se–O(3)	1.733 Å

quently is more easily cut off the radical. Therefore, on x-irradiation, the radical SeO_2^- is formed with O(1) and O(2).

The EPR spectra can be described by the spin Hamiltonian

$$\mathcal{H}=\vec{H}\cdot\vec{\mathbf{g}}\cdot\vec{S}+\vec{S}\cdot\vec{A}_{Se}\cdot\vec{I}_{Se}+\vec{S}\cdot\vec{A}_p\cdot\vec{I}_p \ , \qquad (2)$$

where $S=\frac{1}{2}$, $I_p=\frac{1}{2}$, and A_{Se} and A_p are the selenium and proton hyperfine interaction tensors and $|A_{Se}| >> |A_p|$. Selenium has two isotopes, ^{77}Se (7.58 at.% natural abundance) which has spin $\frac{1}{2}$ and ^{76}Se which has spin zero. Thus, the spectrum has a strong central part resulting from the more abundant nonmagnetic ^{76}Se isotope and satellites which arise from the hyperfine splitting of the ^{77}Se isotope. The ratio between the intensities of the central lines and the satellites is in very good agreement with the calculated number 24.3. The room temperature X-band spectrum in a general orientation is shown in Fig. 2. The lines have a Lorentzian shape and saturate homogeneously down to 77 K.

For H contained in any one of the crystallographic planes *ab*, *ac*, or *bc* the spectrum shows only two central lines and two satellites on each side. The angular variation of the position of the central lines is shown in Fig. 3. Figure 4 shows the shift of each satellite line with respect to its corresponding central line. The magnetic field H was measured by proton NMR and the precision in the relative position of the lines is better than 0.5 G. Corrections were made for changes of the microwave frequency, so that it can be considered fixed at 9003 MHz. The crystal orientation is believed to be precise to within 1°. The dashed lines in both Figs. 3 and 4 are best fits with the spin Hamiltonian.

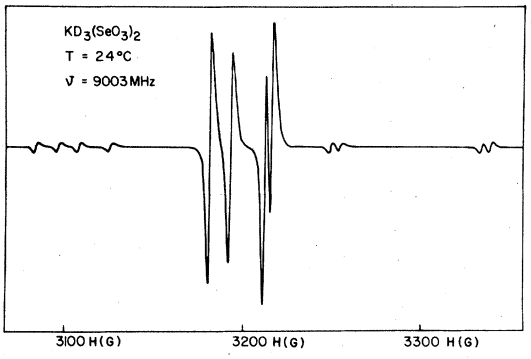

FIG. 2. Room-temperature X-band EPR spectrum of SeO_2^- center in DKTS in a general orientation. The central group of strong lines is due to spinless ^{76}Se. The small lines are due to less abundant ^{77}Se (spin $\frac{1}{2}$).

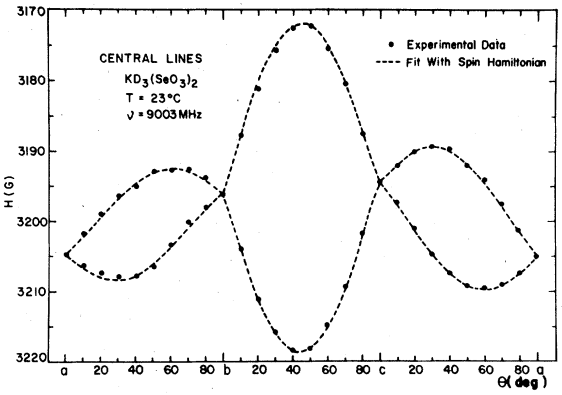

FIG. 3. Angular variation of central lines of SeO_2^- center at 23 °C.

Table II shows the eigenvalues and eigenvectors of the tensors $\vec{\mathbf{g}}$ and $\vec{A}_{Se}$ for site 1 at room temperature. The cosine directors of $\hat{e}_1$, $\hat{e}_2$, and $\hat{e}_3$ with respect to the crystal axes are given in Table III; $\hat{e}_1$ lies along O(1)–O(2), $\hat{e}_2$ is perpendicular to the O(1)–O(2)–Se plane, and $\hat{e}_3$ is the bisector of the O(1)–Se–O(2) angle.

Comparison of Tables II and III shows that the angle between the principal value g_{xx} and $\hat{e}_3$ is 9.6°, the angle between g_{yy} and $\hat{e}_1$ is 1.1° and the angle between g_{zz} and $\hat{e}_2$ is 9.9°. Thus, within the experimental errors the longest principal axis of $\vec{\mathbf{g}}$ can be considered perfectly aligned with the line which connects the two oxygens of the SeO_2^- radicals. The same result was found for $NaH_3(SeO_3)_2$ by Blinc *et al.*[18] This fact also shows that the irradiation defect is essentially an O_2^- pseudomolecule lying along the

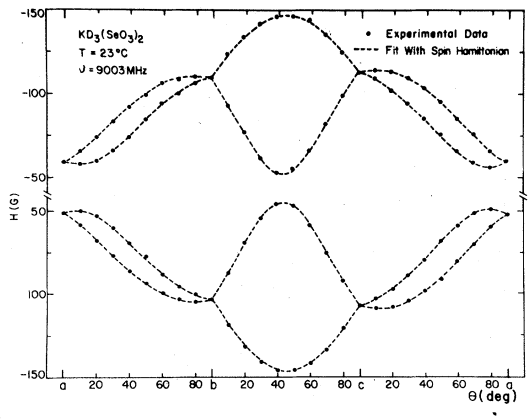

FIG. 4. Angular variation of shift of spin-$\frac{1}{2}$ line with respect to the corresponding central line at 23 °C.

TABLE II. Eigenvalues and direction cosines for $\overleftrightarrow{g}$ and $\overleftrightarrow{A}$ for site 1 at room temperature.

Tensor	Eigenvalues	Direction cosines *a*	*b*	*c*
$\overleftrightarrow{g}$	$g_{xx}=1.9984(3)$	0.124	0.694	0.709
	$g_{yy}=2.0300(3)$	0.289	0.659	−0.694
	$g_{zz}=2.0052(3)$	0.949	−0.291	0.119
$\overleftrightarrow{A}_{Se}$	$A_{xx}=292(2)$G	0.119	0.685	0.719
	$A_{yy}=95(2)$G	0.250	0.682	−0.687
	$A_{zz}=107(2)$G	0.965	−0.242	0.067

O(1)−O(2) direction in the perfect crystal, perturbed by a Se ion on the equatorial plane.

At low temperatures each line of the spectrum splits in two. Thus, in a general orientation of the sample, the spectrum shows eight central lines, and for H contained in one of the planes *ab*, *ac*, or *bc*, it shows four lines. This duplication of the spectrum seems to be caused by the domain twinning of the sample, since it can be suppressed by an external stress $e_4=e_{yz}$.

Figure 5 shows the angular variation of the central lines of the spectrum at $T=-170\,°C$. The eigenvalues and eigenvectors of $\overleftrightarrow{g}$ for the eight sites are shown in Table IV. In the first column the sites are identified by the orientation of the longest principal axis of $\overleftrightarrow{g}$. A surprising fact in the table is the occurrence of two distinct values g_{zz} and g'_{zz} for the magnetically equivalent pairs of sites. The difference is very small, but it is so systematic that the fact deserves some discussion. The powder spectrum, at $-152\,°C$, taken at the Q band for better resolution, shown in Fig. 6, also indicates the existence of two different values for the intermediate principal axis, assigned as g_{zz}. The eigenvalues of g obtained from this spectrum are $g_{xx}=1.9970$, $g_{yy}=2.0291$, $g_{zz}=2.0028$, and $g'_{zz}=2.0046$. The intermediate lines coalesce into one at room temperature, leading to only one value of g_{zz}. From symmetry we could expect the odd-numbered sites to have tensors with different eigenvalues from those of the even-numbered sites, since the symmetry operations of the group C^5_{2h} always bring a site to another of the same parity (i.e., the odd-numbered sites are chemically distinct from the even-numbered ones). The different orientations of the tensors g and g' for each pair of sites must be attributed to the domain twinning of the sample. Examining expression (1) for the free energy we see the spontaneous values of P_2, P_3, σ_5, and σ_6 are zero, and consequently in the absence of external stress the free energy is invariant with respect to a simultaneous change in the signal of Q and σ_4. Thus, all

TABLE III. Cosine directors of SeO_3 axes with respect to the crystal axes; $\hat{e}_1$ lies along O(1)−O(2), $\hat{e}_2$ is perpendicular to the O(1)−O(2)−Se plane, and $\hat{e}_3$ is the bisector of the O(1)−Se−O(2) angle. Calculated from room-temperature data for DKTS in Ref. 6.

	a	*b*	*c*
$\hat{e}_3$	0.263	0.644	0.718
$\hat{e}_1$	0.272	0.665	−0.696
$\hat{e}_2$	0.929	−0.369	−0.009

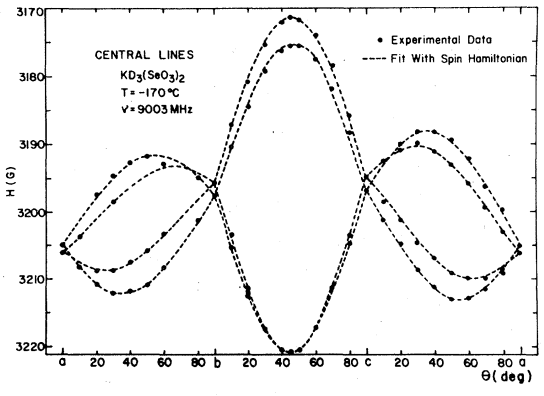

FIG. 5. Angular variation of central lines of SeO_2^- center at $-170\,°C$. The small splittings are due to rotations of SeO_3 groups in opposite directions at low temperatures (compare with Fig. 3).

TABLE IV. Eigenvalues and direction cosines for $\overleftrightarrow{g}$ and $\overleftrightarrow{A}$ for all sites at $-170\,^{\circ}C$. g and g' refer to sites in opposite domains.

Site	g_{ii}	Direction cosines a	b	c
1,7	$g_{xx}=1.9970(5)$	0.125	0.679	0.724
	$g_{yy}=2.0302(5)$	0.372	0.644	−0.669
	$g_{zz}=2.0036(5)$	0.921	−0.346	0.182
	$g'_{xx}=1.9970(5)$	0.120	0.691	0.713
	$g'_{yy}=2.0306(5)$	0.237	0.676	−0.698
	$g'_{zz}=2.0052(5)$	0.964	−0.255	0.079
3,5	$g_{xx}=1.9971(5)$	−0.101	0.685	0.721
	$g_{yy}=2.0308(5)$	0.390	−0.639	0.663
	$g_{zz}=2.0030(5)$	−0.915	−0.340	0.215
	$g'_{xx}=1.9970(5)$	−0.123	0.689	0.714
	$g'_{yy}=2.0309(5)$	0.256	−0.672	0.695
	$g'_{zz}=2.0049(5)$	−0.959	−0.268	0.094
2,8	$g_{xx}=1.9978(5)$	0.068	−0.694	0.716
	$g_{yy}=2.0300(5)$	−0.391	0.641	0.661
	$g_{zz}=2.0031(5)$	0.887	0.449	0.099
	$g'_{xx}=1.9980(5)$	0.099	−0.696	0.711
	$g'_{yy}=2.0299(5)$	−0.255	0.673	0.694
	$g'_{zz}=2.0050(5)$	0.962	0.250	0.111
4,6	$g_{xx}=1.9976(5)$	0.183	0.655	−0.732
	$g_{yy}=2.0298(5)$	0.388	0.637	0.667
	$g_{zz}=2.0035(5)$	−0.904	0.404	0.140
	$g'_{xx}=1.9978(5)$	0.171	0.677	−0.716
	$g'_{yy}=2.0299(5)$	0.248	0.651	0.718
	$g'_{zz}=2.0051(5)$	−0.952	0.302	0.058

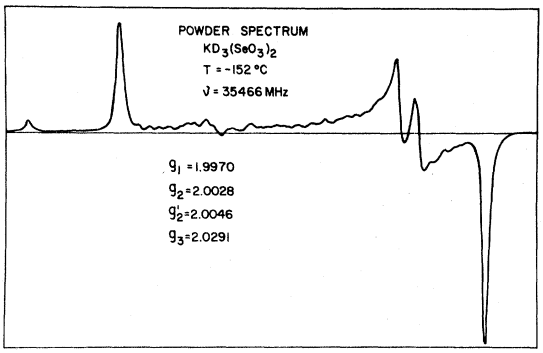

FIG. 6. Q-band powder spectrum of SeO_2^- center at low temperature. The splitting of the central line indicates the existence of two chemically nonequivalent sites.

scalar properties of the crystal should be the same for both domains in contrast to our observations, which suggest that scalar properties of the opposite domains are not exactly the same. This may be an evidence that DKTS is a nonferroelectric pyroelectric. Shuvalov *et al.*[1] have observed previously a weak pyroelectricity in KTS, not confirmed by Makita *et al.*[12]

Since the $\overleftrightarrow{g}$ tensor is nearly axial, there is poor precision in the determination of the direction of the shorter principal axes g_{xx} and g_{zz}. However, the principal axis g_{yy} is very precisely oriented, and its direction can be used as a precise probe for rotations of the SeO_2 radicals, since, as we have already shown, the orientations of the O(1)–O(2) pair in the SeO_2^- defect and in the SeO_3 group are the same. Table V lists the direction cosines of the rotation axes with

TABLE V. Rotation of SeO_2^- radical at different sites at $-170\,°C$.

Site	Angle between g_{yy} and g_{yy}'	Direction cosines of rotation axis a	b	c
1,7	8.1°	0.00	0.71	0.71
3,5	8.1°	0.00	0.71	0.71
2,8	8.2°	0.00	0.72	−0.70
4,6	8.6°	0.15	−0.76	0.64

respect to crystal axes and the angles between g_{yy} and g_{yy}' for the four magnetically distinct sites. Since the radicals rotate in opposite directions for the two domains, the angle of rotation of each radical is half the value seen in the table. Thus, we can conclude that the pair O(1)–O(2) rotates 4.1° in relation to its orientation at room temperature. This is a rather large rotation compared with the rotation of the crystallographic axes b and c related to the spontaneous strain σ_4. At $T = 170\,°C$ Iwata *et al.*[17] found a rotation of 0.8° for those axes in DKTS.

Figure 7 shows the variation of the splitting at the Q band of one central line and one satellite for H on the plane ab, displaced from b by 25° (direction of maximum splitting). Near T_c the splitting was determined by computer fitting the spectral lineshape with Lorentzians. In the X band the splitting is a factor of 3.5 smaller. This fact and the near coincidence of the splitting of the central line and of the satellites show that $\vec{A}_{Se}$ in this direction is nearly constant with temperature. The temperature dependence of the splitting can be described by a critical exponent $\frac{1}{2}$

$$\Delta H \propto (T_c - T)^{1/2} \ . \tag{3}$$

Hence the splitting is proportional to the order parameter.

In addition to the lines already described, the EPR spectra of irradiated KTS and DKTS show very weak lines in the immediate vicinity (less than 3 G apart) of the central line and of the satellites. These weak lines follow the main lines as the crystal orientation is

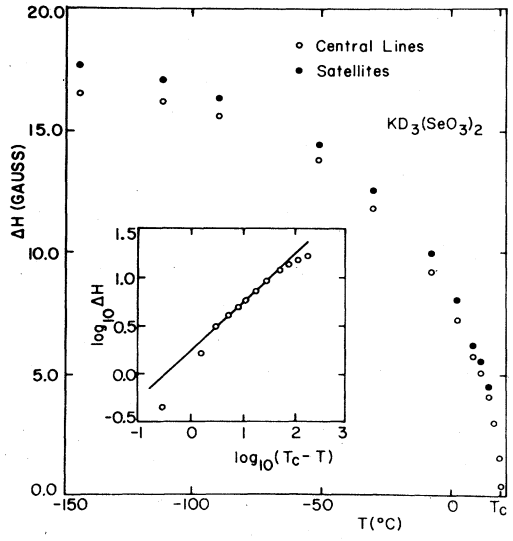

FIG. 7. Temperature dependence of the splittings of central line and satellite measured in orientation of maximum splitting. Insert shows that the splitting is proportional to $(T - T_c)^{1/2}$ at temperatures near T_c.

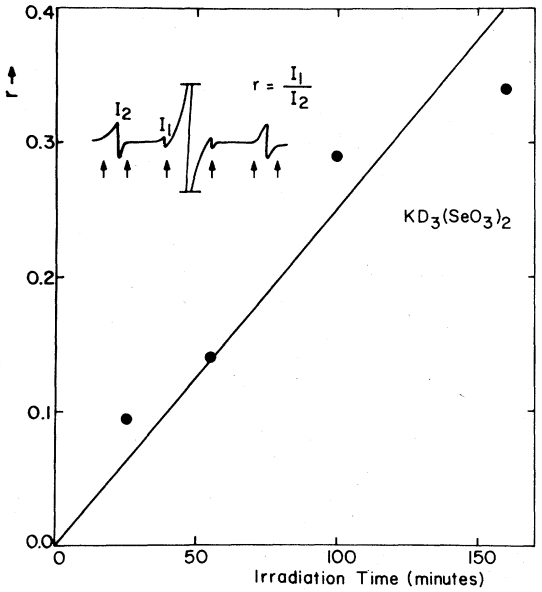

FIG. 8. Increase of intensity of lines due to associated centers with irradiation time.

changed, and their intensities seem to be proportional to the intensities of the lines which they border. It was impossible to determine the detailed angular dependence of these lines because they hide below the normal lines for many orientations. The ratio of intensities of the small satellites and the normal lines was studied as a function of irradiation time. Figure 8 shows that the ratio of the intensity of one of the weak lines around the central line to the intensity of the hyperfine line grows approximately linearly with irradiation time. Our interpretation is that these lines are due to associated SeO_2^- radicals. The density of the coupled centers is expected to be proportional to the square of the density of normal centers and this implies the linear increase of the ratio of intensities with irradiation time shown in Fig. 8. The significant occurrence of coupled SeO_2^- centers in KTS and DKTS results from the exceptionally high rate of formation of these defects by x and γ irradiation. From the graph in Fig. 8 it can be calculated that after 1 h of irradiation of DKTS, under our experimental conditions, approximately 0.5 at.% of the SeO_2^- radicals formed are coupled.

III. CONCLUSIONS

The tensors $\bar{\mathbf{g}}$ and $\bar{\mathbf{A}}_{Se}$ of the SeO_2^- center in DKTS were accurately determined at room temperature, and four magnetically distinct sites were found which transform to each other according to the symmetry operations of the D_{2h} group. Each site generates two distinct sites at low temperatures which correspond to rotations in opposite directions with respect to the room-temperature orientations. It was possible to obtain the value of the rotation angle (4.1° at 100 K) from the analysis of the spectra.

The changes in the EPR spectrum of DKTS (and KTS) have their onset at T_c. Above T_c, up to the melting point there are no perceptible changes in the spectrum. This is in contrast to what happens in KH_2AsO_4 (KDA) and KD_2AsO_4 (DKDA), where the low-temperature symmetry is seen up to a temperature T^* well above T_c, due to low-frequency fluctuations (central peak) of the order parameter.[22] Two kinds of central peaks were reported in KTS: one completely static,[23] interpreted as resulting from the critical behavior of dislocations[24] and one dynamic,[25] presumably intrinsic. The absence of central peak type effects in the EPR measurements indicates that the orientation of the SeO_3 groups does not respond to local fluctuations of short correlation length (small clusters) in the occupation statistics of the protons or deuterons.

The splitting of the EPR lines due to domain twinning was measured at a given angle and it is proportional to $(T_c - T)^{1/2}$, except perhaps very close to T_c, where the splitting is difficult to measure accurately. Thus, the splitting is taken as proportional to the order parameter Q. This allows us to conclude that the rotation of the g tensors is proportional to the order parameter. Using the larger axis of g (g_{yy}), which is aligned in the direction O(1)–O(2), we see that this direction rotates around the axes $(0, \pm\sqrt{2}/2, \pm\sqrt{2}/2)$. Inspection of the correlations of the four magnetically distinct SeO_2^- groups indicates that the distortion transforms according to the B_{3g} mode of the D_{2h} group, and thus has the same symmetry as the order parameter. Thus, the molecular rotations can be bilinearly coupled to the order parameter and the shear strain σ_4 in the bc plane. This bilinear coupling is in complete agreement with the critical exponent $\frac{1}{2}$ found for the molecular rotation.

Finally, there is some evidence that the corresponding sites in opposite domains are not exactly equivalent at low temperature. Thus, the opposite domains may have scalar properties which are not completely equal. This may be considered as a reinforcement of observation of pyroelectricity in KTS by Shuvalov *et al.*[1]

Note added in proof. A recent inelastic neutron scattering study[26] demonstrates the existence of a coupling between the soft acoustic phonon and the hydrogen motion.

ACKNOWLEDGMENTS

This work was partially supported by FINEP (Brazil), CNPq (Brazil), CNEN (Brazil), and IAAE (Vienna).

[1]L. A. Shuvalov, N. R. Ivanov, and T. K. Sitnik, Sov. Phys. Crystallogr. 12, 315 (1967).
[2]N. R. Ivanov, L. A. Shuvalov, and N. V. Gordeeva, Sov. Phys. Crystallogr. 13, 145 (1968).
[3]N. R. Ivanov, L. A. Shuvalov, H. Schmidt, and E. Stolp, Izv. Akad. Nauk. SSSR 39, 933 (1975).
[4]F. Hansen, R. G. Hazell, and S. E. Rasmussen, Acta Chem. Scand. 23, 2561 (1969).
[5]T. Yagi and I. Tatsuzaki, J. Phys. Soc. Jpn. 26, 865 (1969).
[6]M. S. Lehmann and F. K. Larsen, Acta Chem. Scand. 25, 3859 (1971).
[7]B. Prelesnik, R. Herak, Lj. Manojlovic-Muir, and K. W. Muir, Acta Crystallogr. Sect. B 28, 3104 (1972).
[8]Y. Makita and F. Sakurai, Phys. Lett. 55A, 435 (1976).
[9]Y. Makita, T. Yagi, and I. Tatsuzaki, Phys. Lett. 55A, 437 (1976).
[10]Y. Makita, F. Sakurai, and Y. Yamauchi, Ferroelectrics 17, 395 (1977).
[11]Y. Makita, F. Sakurai, T. Osaka, and I. Tatsuzaki, J. Phys. Soc. Jpn. 42, 518 (1977).
[12]Y. Makita, Y. Yamauchi, and S. Suzuki, J. Phys. Soc. Jpn. 43, 181 (1977).

[13]R. Pick (private communication).
[14]R. Blinc, B. Zěks, and A. S. Chaves (unpublished).
[15]N. A. Sergeev and O. V. Falaleev, Zh. Strukt. Khim. 15, 205 (1974).
[16]Y. Iwata, N. Koyano, I. Shibuya, and M. Togunaga, J. Phys. Soc. Jpn. 47, 922 (1979).
[17]J. C. Machado da Silva, A. S. Chaves, R. Gazzinelli, G. M. Ribeiro, R. Blinc, P. Cevc, and R. Srinivasan, J. Phys. Soc. Jpn. 47, 1021 (1979).
[18]R. Blinc, S. Poderaj, M. Schara, and J. Stepisnik, J. Phys. Chem. Solid 27, 1391 (1966).
[19]R. Blinc, Adv. Magn. Reson. 3, 195 (1968).
[20]N. A. Sergeev and O. V. Falaleev, Izv. Akad. Nauk. SSSR 39, 63 (1975).
[21]R. J. Cook, J. R. Rowlands, and D. H. Whiffen, Mol. Phys. 8, 195 (1964).
[22]R. Blinc, P. Cevc, and M. Schara, Phys. Rev. 159, 411 (1967).
[23]T. Yagi, H. Tanaka, and I. Tatsuzaki, Phys. Rev. Lett. 38, 609 (1977); J. Phys. Jpn. 41, 717 (1976).
[24]A. S. Chaves and R. Blinc, Phys. Rev. Lett. 43, 1037 (1979).
[25]J. Slak, B. Lózar, R. Blinc, and L. A. Shuvalov (unpublished).
[26]Y. Noda, R. Youngblood, G. Shirane, and Y. Yamada, J. Phys. Soc. Jpn. 48, 1576 (1980).